Effect of Filler Geometry on Viscoelastic Damping of Graphite/Aramid and Carbon Short Fiber-Filled SBR Composites: A New Insight

S. Praveen,[1] B. C. Chakraborty,[2] S. Jayendran,[2] R. D. Raut,[2] S. Chattopadhyay[1]

[1]Rubber Technology Center, Indian Institute of Technology, Kharagpur 721 302, India
[2]Naval Materials Research Laboratory, Shil, Badlapur Road, Anandnagar, Mumbai 421506, Maharashtra, India

ABSTRACT: An investigation on the effect of filler geometry/shape on the dynamic mechanical properties of polymers was conducted. The viscoelastic damping matrix chosen was SBR and the fillers chosen were graphite, aramid, and carbon short fibers. The study was conducted by taking a control base compound of 20 parts N330 carbon black-filled styrene butadiene rubber (SBR). Dynamic mechanical thermal analyzer was used to investigate the viscoelastic damping of the rubber composites at low dynamic strain levels. Compressive hysterisis at moderate degree of strain were evaluated for all the composite samples to probe into their high strain static damping properties. SEM was used to investigate the matrix-fiber interaction and distribution of the fillers. Investigations demonstrated that the matrix-filler interface plays a major role in energy dissipation. The amount of interface was analyzed by considering the half height width of tan δ peak. Fiber matrix interaction parameter was calculated from the tan δ_{max} values for matrix and composite. It was observed the interaction parameter and the low strain tensile stress values register similar trend. Aramid short fibers were most effective in more energy dissipation than other fillers under consideration. © 2008 Wiley Periodicals, Inc. J Appl Polym Sci 111: 264–272, 2009

Key words: SBR; aramid short fiber; carbon short fiber; graphite; flake like fillers; dynamic mechanical properties; damping

INTRODUCTION

Pristine rubber is an excellent sound and vibration absorber but has poor resistance to abrasion and rapidly degrades especially when exposed to UV light. To produce a material with acceptable mechanical and environmental resistance for critical applications, the rubber must be reinforced, normally with carbon black fillers. While improving the mechanical and environmental resistance of the rubber, this reinforcement has a negative effect on the damping or sound absorption of the rubbers.[1] It is therefore an advantage for these materials to be able to use as little reinforcement as possible, concomitant with acceptable mechanical properties and UV and weather resistance.

Elastomers-filled with short fibers and graphite are receiving attention because of the ability to tailor their vibration damping potential. Viscoelastic constrained layers are effective in reducing vibrations, but for obvious reason cause a reduction in rigidity.[2] Constrained layer damping may also be effective only over a relatively narrow frequency range.[3] Fillers like graphite, short carbon, and aramid fibers have anisotropic structures. Graphite has flake-like structure while the short fibers have cylindrical rod like structures. To achieve high damping and stiffness simultaneously over a broad frequency range, fiber/graphite reinforced elastomer composite material can be developed. Graphite, aramid, and carbon short fibers are extremely stiff relative to most elastomers; hence, a large stiffness mismatch exists in the interphase region that enables good storage of strain energy and enhances shear displacements mechanisms. The increased damping was indicated as probably because of a "micro-mechanical constrained layer damping mechanism,"[2] where relative motion between the reinforcing fibers introduced additional shear into the matrix. The layered structure of graphite facilitates enhanced damping because of large internal surface area involved. This will contribute to higher energy losses because of internal friction between the layers.[4]

Dynamic mechanical test methods have been widely employed for investigating the viscoelastic behavior of polymers for determining their stiffness and damping characteristics for different applications. The dynamic properties of polymeric materials are of considerable practical significance when determined over a range of temperature and frequencies. To obtain a good correlation between the dynamic

Correspondence to: S. Chattopadhyay (santanuchat71@yahoo.com).

property of the material and its performance in the field, the laboratory condition should simulate the actual application conditions as closely as possible. For the best correlation, the following factors have to be carefully considered, namely, time, temperature, and strain level of the laboratory measurement, and also use of a relevant dynamic viscoelastic property. Time temperature superposition principle is often used to convert the actual field condition in a laboratory measurable rate and temperature. Strain level is also important because most filler-reinforced materials show nonlinear viscoelastic properties, and their dynamic properties vary with level of strain.

The main goal of this work is to evaluate the effect of the incorporation of graphite, carbon and aramid short fibers to rubber to form polymer composites with optimum damping at both high and low strain levels along with good strength properties.

EXPERIMENTAL

Materials used

KOSYN SBR 1502 with 23% styrene Mooney viscosity of $ML_{1+4} = 54$ at 100°C, was procured from KOSYN, Korea. Chopped aramid fiber D1189 of length 1.5 mm, aspect ratio 250 was procured from Teijin Twaron, the Netherlands. Chopped carbon fiber of length 1.5 mm and aspect ratio 250 was supplied by Polymer technologies Ltd., Singapore. Graphite was procured from Cabot, USA, having specific gravity = 2.2, 325 mesh, iodine no = 11, 95% minimum carbon content. N330 carbon black was procured from Philips Carbon Black Ltd., Calcutta, India. Other rubber chemicals were of analytical grade and were purchased from local suppliers. Sample designations are given in Table I.

Preparation of rubber composites

Rubber composites based on graphite, carbon, and aramid short fibers were prepared by mixing in conventional laboratory two roll mixing mill. During the mixing of carbon and Kevlar short fibers, the short fibers were incorporated before the addition of carbon black. Graphite was incorporated by usual rubber mixing process. A control base compound of 20 parts N330 carbon black-filled styrene butadiene rubber (SBR) with conventional sulfur based cure systems was used in all compositions. Optimum cure time (OCT) for the composites were determined by Moving Die Rheometer (MDR 2000, Alpha Technologies, USA) at 150°C. 2-mm-thick sheets of composites were compression molded at their respective optimum cure times at 5 MPa pressure and temperature of 150°C at OCT.

TABLE I
Filled SBR Composites and Their Designation

Designation	Composition
SBR	Styrene butadiene rubber
KF	Aramid short fiber
CF	Short carbon fiber
G	Graphite
HAF 20	20-phr N330
G15	Graphite 15 phr with 20-phr N330 black
G30	Graphite 30 phr with 20-phr N330 black
G55	Graphite 55 phr with 20-phr N330 black
KF 10	10 phr aramid fiber with 20-phr N330 black
KF 20	20-phr aramid fiber with 20-phr N330 black
KF 30	30-phr aramid fiber with 20-phr N330 black
CF 10	10-phr carbon short fiber with 20-phr N330 black
CF 20	20-phr carbon short fiber with 20-phr N330 black
CF 30	30-phr carbon short fiber with 20-phr N330 black

Mechanical properties

Tensile specimens were punched out from the molded sheets using ASTM Die- C. The tests were carried out as per the ASTM D-412 methods in a Universal Testing machine (Hounsfield 50K). Tensile properties reported here are the averages of five samples. Compressive hysterisis analysis was conducted on cylindrical specimens of dimensions 29.5 mm × 12.5 mm thick. The test was conducted on the Universal Testing Machine (Hounsfield 50K, UK) at a crosshead speed of 12 mm/min. The samples were subjected to 2-mm compression and load was released in controlled rate at 25°C. The average of two tests is reported here.

SEM analysis

To study the developed morphology of the short fiber rubber composites, scanning electron microscopy (SEM) examination was performed on gold coated surfaces of the cryo-fractured samples by the use of a JSM 5800 microscope (JEOL, Japan). The accelerating voltage of the beam was 15 kV.

Dynamic mechanical properties

The dynamic mechanical thermal analysis was conducted using rectangular samples with dimensions 25 mm × 10 mm × 2 mm thick on DMA machine of GABO, Germany, in tension mode. Two different types of experiments were conducted (a) dynamic temperature sweep test at a frequency of 1 Hz in the temperature range −80 to + 50°C with 0.05% strain. (b) Temperature-frequency sweep test. The tests were conducted from −80 to + 50°C over a frequency range of two decades (0.5–50 Hz) with a strain of 0.05%. Storage modulus (E′), loss modulus (E″), and loss tangent (tan δ) were measured as a function of temperature for all the samples under

TABLE II
Tensile Properties of Graphite-Filled SBR

| Properties | Graphite loading | | | |
	G15	G30	G55	HAF 20
Tensile strength, MPa	7.3	13.4	8.3	8.6
Elongation at break, %	315	511	278	261
Stress at 100% elongation, MPa	2.43	2.70	3.40	2.5

identical conditions. The temperature corresponding to tan δ_{max} was taken as the glass-transaction temperature (T_g).

RESULTS AND DISCUSSION

Tensile properties

The tensile properties of graphite-filled SBR composite are reported in Table II. Addition of 15-phr graphite to the control formulation (N330-filled SBR) showed a tensile strength of 7.3 MPa. The tensile strength increased to a maximum value of 13.4 MPa for 30-phr Graphite loading which subsequently decreases with further loading. Graphite being semi-reinforcing filler, the higher loading leads to dilution effect resulting in decrease in the strength. However, the modulus value showed an increase from 2.5 MPa of control compound to 3.4 MPa (following Guth Gold equation) after addition of as high as 55-phr graphite.

The stress strain plot of short Kevlar fiber (KF)-filled control SBR showed a stick-slip type of failure (Fig. 1), presenting poor fiber matrix adhesion it higher strains. However, at low strain levels, SBR shows good adhesion with fiber. Short carbon fiber (CF)-filled compounds, on the other hand, showed a stress–strain behavior similar to that of conventional carbon black-filled compounds, indicating its better interaction with the matrix. Kevlar-filled compounds showed higher strengths than carbon fiber-filled compounds (Table III)—a maximum value of 10.6 MPa for 20-phr KF loading was achieved. Elongation at break dropped drastically for higher loadings. The stress at 100% elongation was also higher for KF compounds. CF-filled compounds showed stress–strain behaviors similar to that of graphite-filled compounds.
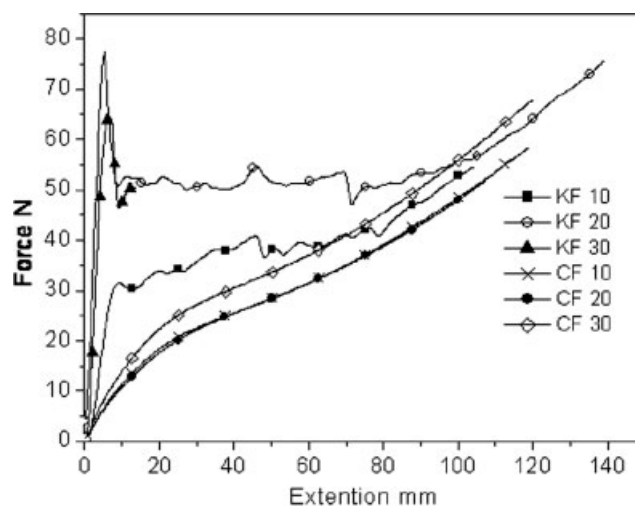
Figure 1 Tensile behavior of short fiber—SBR composites.

Morphology studies with SEM

SEM fractographs revealed considerable breakage of short carbon fiber during mixing. Aramid fibers remained intact during mixing. SEM pictures also reveal good adhesion between carbon fiber and rubber matrix and weak adhesion with aramid fibers and the matrix. The interfacial failure between the aramid fiber and SBR matrix observed in Figure 2 may be attributed to very high level of shear strain experienced by the interface during the cryo-fracture. The localized damage at the aramid fiber end is believed to be caused by the radial stress upon fracture. The SEM fractographs also show a significant difference in the surface topography of aramid and carbon short fibers. The surface of the aramid fibers appears to have undergone shear deformation during mill mixing. Because of the higher toughness of aramid, the fiber does not undergo fracture and the shear stresses are completely transferred on to the fiber surface. On the other hand, carbon fiber is more brittle by nature and because of the breakage the level of shear stress experienced by the carbon fiber is less as the stress transfer length is much smaller than that of aramid. From Figure 2c, it can be observed that the carbon fiber has broken down to approximately 20 μm from its original length of 1.5 mm.

TABLE III
Tensile Properties of Short Fiber-Filled SBR

| Properties | Kevlar short fiber (phr) | | | Carbon Short Fiber (phr) | | |
	10	20	30	10	20	30
Tensile strength, MPa	9.2	10.6	9.7	7.8	7.1	8.6
Elongation at break, %	252	295	25	222	211	223
Stress at 100% elongation, MPa	5.3	7.1	–	3.3	3.8	4.4
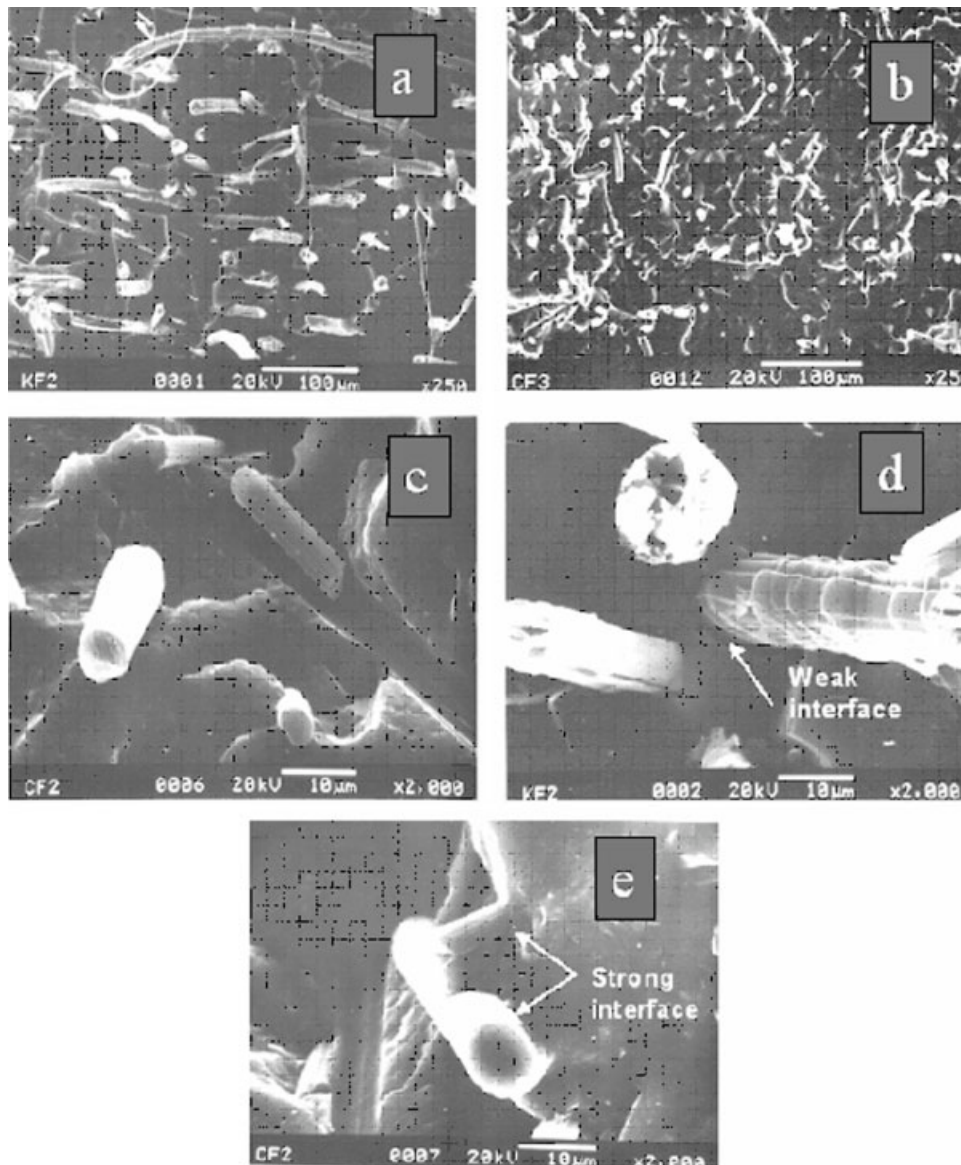
Figure 2 SEM fractographs of short fiber SBR composites. (a) Aramid fibers with out breakage; (b), (c) broken carbon fibers at different magnifications (d) demonstrating weak adhesion between aramid fiber and matrix (e) showing good adhesion between carbon fiber and matrix.

Dynamic mechanical properties

Dynamic temperature sweep

DMA is an effective tool to determine the glass transition temperature, T_g (dynamic) and damping (dissipation factor). The dynamic T_g is defined as the temperature at which (i) maximum of the tan δ occurs or (ii) maximum change of E″ occurs or (iii) the middle point of E′ versus temperature curve or (iv) the region where E′ increases with increasing frequency at constant temperature.[4]

The dynamic mechanical properties of all the composites were compared with that of control SBR compound in this section. The variation of tan δ and storage modulus (E′) with temperature for graphite-SBR composites can be seen in (Fig. 3). The tan δ

peak height was reduced, when compared with the control SBR. The peak height remains almost constant for all loadings of graphite. The lack of chemical functional groups on the graphite surface results in weak polymer filler interactions,[5] which are insufficient to immobilize the polymer molecules from taking part in relaxation process. The width of tan δ remained indifferent with graphite loading.

The basic concept of damping involves the absorption of external energy through molecular friction. The layered structure of graphite is attractive for damping because of the large internal surface area involved.[6–8] The relative motion between layers produces extra friction because of shear, which contributes toward additional energy dissipation.[9] This energy dissipation is in addition to that of damping
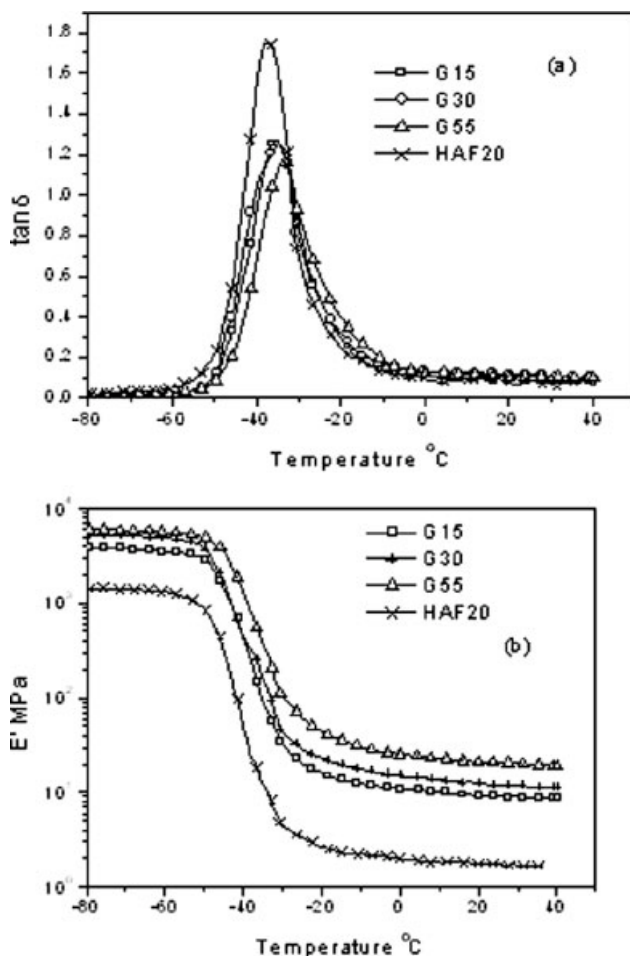
Figure 3 Variation of (a) tan δ and (b) dynamic storage moduli with temperature for graphite-filled SBR.

the combination of the hydrodynamic effects of the fibers embedded in a viscoelastic medium and to the mechanical restraint introduced by the filler at the high concentrations, which reduce the mobility and deformability of the matrix.[10] At low temperature, E′ values of the matrix (carbon black-filled rubber) and fiber composite are found to be closer in the rubbery region emphasizing that at low temperature fibers do not contribute much to imparting stiffness to the material. Aramid fiber imparts higher modulus to the matrix compared with carbon fiber. Carbon fiber-filled composites show storage modulus value similar to that of graphite composites. This difference is attributed to the breakage of fiber filaments of chopped carbon fiber during the mixing process in two roll mill as mentioned earlier. Aramid filaments remain intact thus possess higher load bearing capability.

Tan δ is a damping term and the damping peak occurs in the region of the glass transition where the

due to the viscoelastic matrix which is sandwiched between the graphite layers. The storage modulus increases with graphite loading. As the temperature increases from glassy to rubbery stage through the transition, the differences in the modulus values among the composites are more pronounced in the rubbery plateau region. At low temperatures, the E′ values of the composites are found to be close to each other, in the rubbery region the filer loading becomes the deciding factor, as the volume fraction of polymer decrease with increasing filler loading. As a result of this, composite modulus tends to be closer to that of filler rather than the matrix. For low loadings the matrix modulus, which falls drastically from that of glassy modulus, is the deciding factor.

Figure 4 shows the effect of fiber loading on the storage modulus (over range of temperatures) of short carbon fiber and short Aramid fiber-filled SBR composite. Variation in modulus occurs because of the effect of the incorporated fibers. The difference between the moduli of the glassy state and rubbery state is smaller in the composites than that for carbon black-filled sample. This can be attributed to

Figure 4 Variation of storage modulus with temperature (a) carbon short fiber-SBR composites; (b) aramid short fiber-SBR composites.
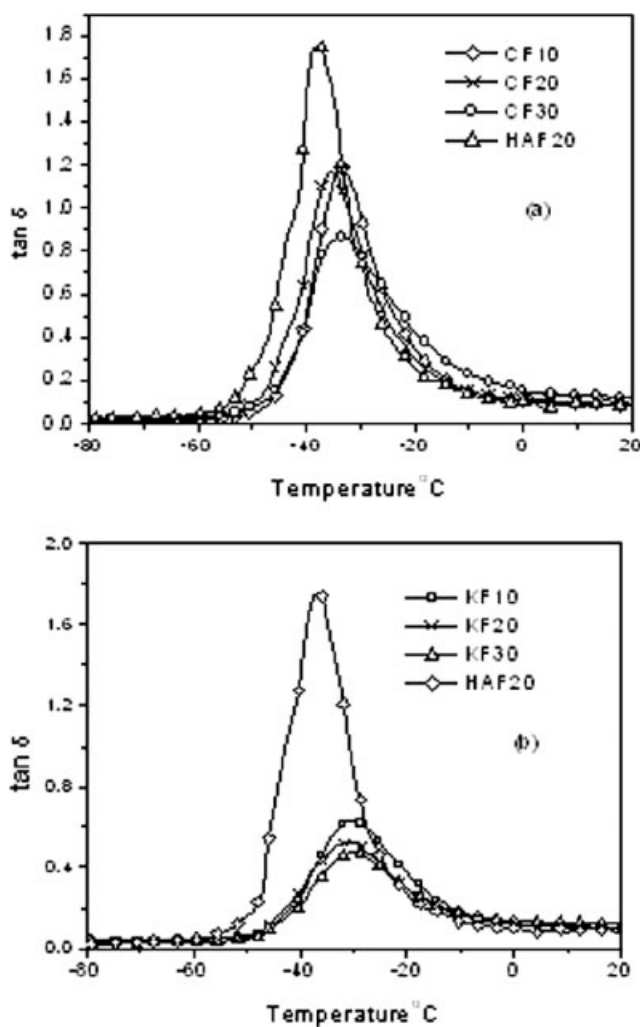
Figure 5 Variation of tan δ with temperature: (a) carbon short fiber; (b) aramid short fiber.

material changes from glassy to a more elastic state. It is associated with the movement of small groups and chains of molecules within the polymer structure—all of which are initially frozen in. In a composite system damping is affected through the incorporation of fibers. This is due to shear stress concentrations at the fiber-matrix interface, in association with the additional viscoelastic energy dissipation in the matrix material.[10]

Figure 5 shows the tan δ versus temperature curves for carbon fiber and aramid fiber composites. Magnitude of the tan δ peak is indicative of the nature of the polymer system. In an unfilled system, the chain segments are free from restraints. Incorporation of fibers reduces the tan δ peak height by restricting the movement of polymer molecules. The addition of aramid fibers showed a positive shift in T_g value compared with carbon fiber. This positive shift in T_g values emphasizes the effectiveness of the aramid fiber as a reinforcing agent, i.e., the high polymer–filler interaction. In addition, the stress

field surrounding the fibers induces the T_g shift. Because of the breakdown of the carbon fiber, the effective interface of carbon fiber with rubber matrix is smaller compared with that of Aramid. The *critical fiber length*[11] of aramid is higher than that of carbon fiber because of the break down of latter during n\mixing. This leads to elevated rank of physical immobilization of the polymer chains in contact with fiber surface leading to a positive shift in T_g. Additionally, the difference in the thermal conductivities of two different fibers may also contribute to the overall shift in T_g. The introduction of filler reduces the magnitude of the tan δ peak. It has been reported that the tan δ peak height is reduced as a greater number of polymer chains is restricted in their movement.[12,13] This observation is strongly supported by the tensile stress strain behavior of aramid fiber composites. DMA is carried out at a very low strain of 0.05%. The tensile graphs show that there is good adhesion between the fiber and SBR matrix up to a strain level of 24%. The tan δ peak value and T_g values are shown in Table IV.

It was also observed that the width of the tan δ peak becomes broader than that of control with increase in fiber loading. At higher fiber content when strain is applied to the composites, the strain is controlled mainly by the fiber in such a way that the interface which assumed to be the more dissipative component of the composites is strained to a lesser extent.[14] This suggests the existence of molecular relaxations in the composites that are not present in the pure matrix. The molecular motions at the interfacial region generally contribute to the damping of the material apart from those of the constituents.[15] Hence the width of tan δ peak is indicative of the increased volume of the interface. Figure 6 shows the variation of tan δ with temperature for SBR composites with 10 phr of individual fillers. Graphite being a semi-reinforcing filler has little interaction with the matrix to affect the relaxation mechanism of matrix. As a result, graphite-filled

TABLE IV
Interaction Coefficient, tan δ_max, Dynamic T_g, Interaction-Coefficient, and Low Strain Modulus of Short Fiber-Rubber Composites

Composite	tan δ_{max}	T_g (°C)	β	Tensile stress at 2% elongation (MPa)
HAF 20	2.1	−36	–	–
CF 10	1.19	−30	6.19	0.32
CF 20	1.16	−30	3.24	0.32
CF 30	0.86	−29	3.04	0.43
KF 10	0.62	−32	10.06	0.48
KF 20	0.52	−32	5.45	2.01
KF 30	0.47	−32	4.00	3.65
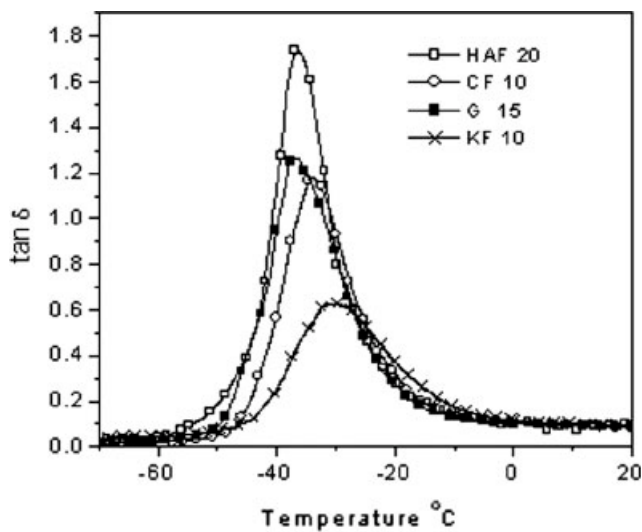
Figure 6 Variation of tan δ with temperature for SBR composites.

system shows the same T_g ($-36°C$) as that of matrix. Where as in the case of short fiber composites, the T_g shifts toward higher temperatures, with aramid showing maximum shift ($-30°C$), indicating better fiber–matrix interaction.

The dependence of fiber reinforcement on tan δ_{max} has been extensively studied by many authors.[16–18] The results depend heavily on the type of fiber and matrix that are used, but a decrease of tan δ_{max} with increasing fiber loading is always detected as can be seen from Figure 5. This decrease is described by eq (1)[19]:

$$(\tan \delta_{max})_c / (\tan \delta_{max})_m = 1 - \beta - V_f \quad (1)$$

where subscripts 'c' and 'm' denote the composite and matrix and β is a coefficient depending on the matrix. From the value of β, the degree of the interaction between fibers and matrix can be estimated. Table IV shows the interaction coefficient and stress strain properties of fiber- elastomer composites. Comparing the β values for these composites with the mechanical properties, it can be found that the tensile stress at 2% elongation scales with β values for these composites. It can be seen that low strain modulus increases with increase in β value. However, in the case of KF 10, the modulus is lesser than expected. This may be due to the higher volume fraction of the matrix, where the matrix modulus is more prominent. When the fiber concentration is lower, the packing of the fibers will not be efficient in the composite. This leads to matrix rich regions and thereby easier failure of the bonding at the interfacial region. When there is closer packing of the fibers, crack propagation will be prevented by neighboring fibers.[10]

Master curve

Time temperature superposition (TTS), one of the most useful extrapolation techniques with a wide range of applications, has been applied to virtually every time dependent mechanical property and every kind of polymers.[20] Many believe[21] that this superposition manifests itself from molecular behavior and, therefore, formulate equations based on the activation energy (E), such as this Arrhenius equation:

$$\ln a_T = \frac{E}{R} \left(\frac{1}{T} - \frac{1}{T_0} \right) \quad (2)$$

where a_T is the horizontal (or time) shift factor, R is the universal gas constant, T_0 is the reference temperature (K), and T is the temperature at which a_T is desired.

Another commonly used empirical equation for TTS is the Williams-Landel-Ferry (WLF) equation, which relates a shift in temperature with a shift in time. This shifting equation is very useful if information is available for only one temperature and information must be computed for other temperatures. Conversely, if information is available at different temperatures, then more precise extrapolations and interpolations can be obtained if we direct high-temperature data to longer times to correspond to lower temperature data. The WLF equation has the following form[22]:

$$\text{Log } a_T = \frac{-17.4 (T - T_g)}{51.6 + T - T_g}. \quad (3)$$

Amorphous polymers obey the superposition principle, i.e., dynamic modulus is a function of temperature as well as frequency. The process of developing a master curve is called the time–temperature superposition. Curves obtained at different temperatures were superimposed by horizontal shifting using the shift factor a_T, covering a very large range of time (inverse of frequency). Such curves made by superposition, using a reference temperature, will be able to cover times outside the range which are not easily accessible by practical experiments. The curve made by superposition is called a *master curve*.

In developing the master curve the reference temperature of 25°C was selected. Figure 7 shows the effect of type of filler (loading 10 parts short fiber versus 15 parts graphite) on the damping behavior (tan δ) of the carbon black-filled SBR over a wide range of frequencies. Graphite showed peak damping at 10 MHz while carbon fiber composite showed peak damping at 0.5 MHz (one and half decade lower than that of graphite). It may be noted that in the dynamic temperature ramp test, conducted at 1 Hz, there was a difference of 4°C between the tan
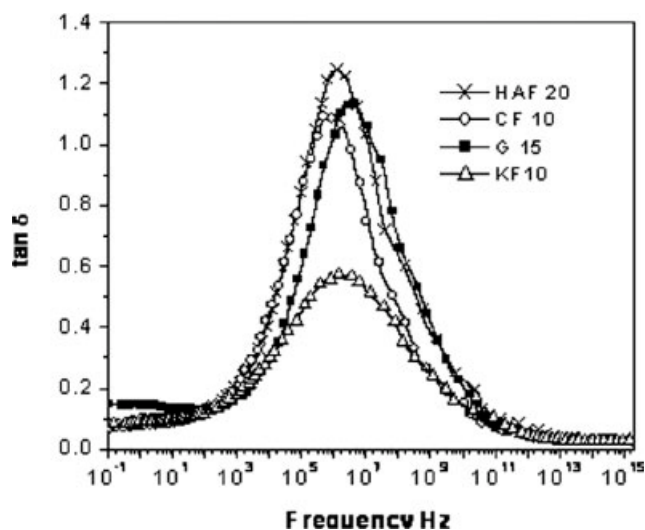
Figure 7 Master curve for graphite and short fiber composites, reference temperature 25°C.

δ_{max} temperature for G15 (-36°C) and CF 10 (-32°C). This difference is reflected in the TTS curves by the shift in tan δ_{max} frequencies. Normally a 5–7°C shift in temperature will lead to a shift of one decade in frequency scale.[3] Aramid-rubber composites showed a broad damping, emphasizing the high level of interface with matrix.

Hysterisis

Historically, tan δ has been most frequently used as a relevant dynamic property of the material for hysteretic energy-loss processes. However, there is no fundamental reason why tan δ should be always chosen because the dynamic property that gives the best correlation depends on the type of deformation applied to the material. Theoretically, the energy loss E_{loss} per cycle of a material under cyclic deformation is described as follows:

$$E_{loss} = \pi \, \varepsilon_0^2 \, E'' = \pi \alpha_0^2 \, D'' \qquad (4)$$

where ε_0 is the strain σ_0 is the stress E' and D'' are the loss modulus and loss compliance, respectively. For constant strain deformation, E_{loss} would be proportional to loss modulus and for constant stress deformation; it would be proportional to the loss compliance.[23]

Table V reveals the compression hysterisis data of rubber composite corresponds to a strain level of 16%. Short fiber-filled composites showed maximum hysterisis. In short fiber composites, the polymer is the only continuous phase. Longitudinal tensile stresses are applied to the fibers through shearing in the matrix. These shearing stresses in the matrix are highest near the ends of the fibers and gradually decrease to zero away from the ends. The tensile loads in the fibers are zero at the ends and gradually increase to a plateau in the central portion of the fibers. Thus the part of the fiber near the ends carries fewer loads than the middle section. The sum of the length of the fiber on each end required for the tensile load to reach its plateau or maximum value which is often called the critical fiber length or ineffective length L_c, since the end portion of the fibers are ineffective in carrying the load. In other wards, a fiber must have a length at least L_c to achieve the maximum tensile stress in the fiber.

Because shearing stresses are induced on to the matrix because of the presence of fiber interface, losses are higher. Aramid short fiber composites registered highest hysterisis energy loss followed by carbon short fiber and graphite. Since the Aramid fiber does not undergo breakage, the critical fiber length is maintained. The highest hysterisis shown by the aramid short fiber composites can be attributed to the larger portion of weak interface region (at higher strain levels) which contributes to the viscoelastic damping of the material apart from those of the constituents.[10] Aramid shows higher losses because of the lesser degree of fiber breakage leading to higher load transfer ability at the interface compared to the carbon fiber which undergoes considerable filament breakage.

TABLE V
Compression Hysterisis Data for SBR-Graphite/Short Fiber Composites

Type of filler	Filler loading (phr)	Storage modulus (MPa)	tan δ peak width at half height (°C)	tan δ at 30°C	tan δ_max	Energy loss/unit volume × 10⁻⁴ MPa	Hysterisis (%)
HAF 20	20	1.73	12	0.08	1.74	10.86	5.8
Graphite	15	9.14	17	0.08	1.26	57.4	21.6
	30	12.26	16	0.12	1.25	115.5	24.0
	55	20.30	15	0.10	1.17	159.3	32.3
Carbon short fiber	10	12.50	15	0.08	1.19	78.5	27.6
	20	16.20	15	0.08	1.16	101.7	29.2
	30	22.30	21	0.12	0.86	210	34.3
Aramid short fiber	10	49.50	22	0.08	0.62	310	37.0
	20	82.20	22	0.10	0.52	645	39.3
	30	166.60	24	0.12	0.47	1569	41.3

The compression hysterisis data (measured by using UTM) were measured at 16% strain and the energy loss per unit volume were (measured from the DMA) calculated at low strain level of 0.05% at ambient temperatures.It is clear from the Table V that Aramid short fiber-filled composites showed higher losses both at high and low strain levels.

CONCLUSIONS

SBR was used to investigate the effect of filler geometry on the damping capability of rubber composites. Study was mainly concentrated on the flake like filler (graphite) and cylindrical rod like filler (Aramid and carbon short fiber). Tensile tests revealed poor adhesion between the aramid fiber and rubber matrix at higher strains and good adhesion at low strains. SEM fractographs, reveled considerable breakage in carbon fiber where as aramid underwent no breakage which largely influenced the resulting dynamic properties. Dynamic mechanical analysis divulged a shift in the T_g toward higher temperature and broadening of the peak in the case of aramid-filled composites. The peak damping decreased considerably after the addition of Aramid fibers. But the width of tan δ peak increased with increase in fiber loading. Tan δ peak height for graphite did not decrease even after higher loadings although there is an increase in the storage modulus value. The width of tan δ remained indifferent with graphite loading. The amount of interface was analyzed by considering the half height width of tan δ peak. Fiber matrix interaction parameter was determined from the tan δ_{max} values for matrix and composite. It was observed the interaction parameter values given an indication of the tensile modulus at low strain levels of such composites. From the temperature - frequency sweep test it is clear that for Graphite and carbon short fiber composites, peak damping shifts toward lower frequency. Aramid displayed peak damping over a broad range of frequencies. Compressive hysterisis and energy loss per unit volume was found to be higher for Aramid fiber composites. Aramid-rubber composites showed better damping both at low and high strain tests. It may be concluded that the damping mechanism in short fiber (cylindrical rod like geometry) composites originates by the transformation of longitudinal stresses to interfacial shear stress between the fiber and SBR matrix, while in a flake like filler like graphite the energy dissipation is predominantly by inter-layer friction.

References

1. Blorkert, S.; Karasalo, I.; Savage, S; Staaf, S; Svensson, S. Technical report, Swedish Defence Agency, 2003.
2. Sharma, A.; Peel, L. D.; Technical Paper, SAMPE Long Beach, CA, 2004.
3. Corsaro, D.; Sperling, L. H. Sound and vibration damping with polymers: 424, ACS Symposium Series, 1990.
4. Geethamma, V. G.; Kalaprasad, G.; Groeninckx, T. S. Composites: Part A 2005, 36, 1499.
5. Schröder, A.; Klüppel, M.; Schuster, R. H. Macromol Mat and Eng 2007, 292, 885.
6. Luo, X.; Chung, D.D.L. Carbon 2000, 38, 1499.
7. Gregory, B.; Hiltner, A.; Baer, E. Polym Eng Sci 1987, 27, 568.
8. Chegodaev, D. E.; Ponomarev, Y. K. Izvestiya Vyssh Uchebn Zaved Aviatsion Tekhn 1993, N2, 63.
9. Azvine, B.; Wynne, R. J.; Tomlinson, G. R. IEEE conference publication, IEE Stevenage, UK 1994, 2, 1296.
10. Pothan, L. A.; Oommen, Z.; Thomas, S. Compos Sci Technol 2003, 63, 283.
11. Nielsen, L. E.; Landel, R. F. Mechanical Properties of Polymers and Composites, 2nd ed.; Marcel Dekker: New York, 1994.
12. Wong, S.; Shanks, R.; Hodzic, A. Compos Sci Technol 2004, 64, 1321.
13. Datta, C. B. D.; Banerjee, A. J Appl Polym Sci 2000, 85, 2800.
14. Ibarra, L.; Macias, M.; Palma, E. J Appl Polym Sci 1995, 57, 831.
15. Dong, S.; Gauvin, R. Poly Comp 1993, 14, 414.
16. Ibarra, L.; Jorda, C. J Appl Polym Sci 1993, 48, 375.
17. Ashida, M. Composites of Polychloroprene Rubber with Short Fibres of Polyethylene Terephthalate and Nylon. Wood head Publishing limited, Abington Hall: Abington, Cambridge, 1996.
18. Kutty, S. K. N.; Nando, G. B. J Appl Poly Sci 1991, 43, 1913.
19. Michio, A.; Noguchi, T. J Appl Polym Sci 1985, 30, 1011.
20. Turi, E. A. Thermal Characterisation of Polymer Materials, 2nd ed.; Academic Press: San Diego, 1997.
21. Aklonis, J. J.; Macknight, E. J. Introduction to Polymer Viscoelasticity; Wiley: New York, 1983.
22. Tajvidi, M.; Falk, R. H.; Hermanson, J. C. J Appl Polym Sci 2005, 97, 1996.
23. Shingo Futamura, RCT 1990, 64, 58.